*Article*

# Theoretical and experimental study on a spirocyclic diethyleneglycol silicon complex

J. Oscar C. Jiménez-Halla,[a] Juvencio Robles,[a,*] Manuel Villanueva,[a] Jorge Cervantes,[a] Gerardo González-García,[a] M. Carmen Salazar-Hernández,[a] Marco A. Leyva-Ramírez,[b] Armando Ramírez- Monroy,[b] J. Alfredo Gutiérrez[a,*]

[a] Universidad de Guanajuato, Facultad de Química, Noria Alta s/n. Guanajuato, Gto., 36050, México.
  Phone and fax: (+52) 473 732 0006 ext. 8111. E-mail: jagutier@quijote.ugto.mx; roblesj@quijote.ugto.mx
[b] Centro de Investigación y Estudios Avanzados del Instituto Politécnico Nacional. Apdo. Postal 14-740,
  México 07000, D.F. México.

**Abstract.** In this paper a joint theoretical and experimental study examines the ability of diethyleneglycol as a ligand to form silicon complexes. Due to the known oxophilia of the silicon atom, it would be expected that in the reaction of this tridentate O,O,O-donor-ligand with a reagent such as $SiCl_4$, the corresponding bis-chelate, hexacoordinated neutral silicon complex may be formed. However, a spirocyclic tetracoordinated silicon bis-chelate complex was isolated and no evidence of formation of any hypervalent alkoxysilane was observed. The tetracoordinated compound, 1,4,7,9,12,15-Hexaoxa-8-silaspiro[7.7]pentadecane (8CI,9CI), was crystallized in hexanes from an extract of the product of the aforementioned reaction in methylene chloride and its crystal structure has been determined by X-ray diffraction ($C_8H_{16}O_6Si$; orthorhombic; $a = 9.2892(3)$, $b = 9.5845(3)$, $c = 12.3748(4)$ Å; space group $P2_12_12_1$; $Z = 4$). From the same reaction, two other oligomeric tetracoordinated silicon compounds were detected spectroscopically. Furthermore, Density Functional calculations at the BP86/TZ2P level were performed for the bis-chelate compound. We obtained the condensed Fukui functions as well as theoretical NMR chemical shifts to rationalize why the diethyleneglycol acts only as a dianionic, bidentate ligand towards silicon. Our DFT results indicate that the tetracoordinated Si complex is a stable molecule (minimum energy point) whereas the hexacoordinated species is a first-order saddle point (transition state). These results are in agreement and rationalize the experimental findings.
**Key Words**: Silicon, Diethyleneglycol, Hypervalent compounds, Density functional calculations, Fukui function.

**Resumen.** Mediante un estudio teórico y experimental se analizó la capacidad ligante del dietilenglicol para formar complejos con el átomo de silicio. Debido a la bien conocida oxofilia del silicio, se esperaría que la reacción de este ligante tridentado O,O,O-donador con un reactivo tal como el SiCl4 daría lugar a la formación del correspondiente complejo bisquelato hexacoordinado neutro de silicio. En su lugar se aisló un complejo espirocíclico bisquelato tetracoordinado y no hubo evidencia de la formación de algún alcoxisilano hipervalente. El compuesto tetracoordinado, 1,4,7,9,12,15-Hexaoxa-8-silaespiro[7.7]pentadecano (8CI,9CI) fue cristalizado en hexano a partir de un extracto del producto de reacción en cloruro de metileno, y se determinó su estructura cristalina mediante difracción de rayos X de cristal único ($C_8H_{16}O_6Si$; ortorrómbico; $a = 9.2892(3)$, $b = 9.5845(3)$, $c = 12.3748(4)$ Å; grupo espacial $P2_12_12_1$; $Z = 4$). En la misma reacción se detectaron espectroscópicamente dos compuestos de silicio tetracoordinado y oligomérico. También se llevaron a cabo cálculos de Funcionales de la Densidad (DFT) al nivel BP86/TZ2P para el compuesto bisquelato. Se obtuvieron las funciones condensadas de Fukui así como los desplazamientos químicos teóricos de RMN para racionalizar porqué el dietilenglicol actúa como un ligante bidentado dianiónico frente al silicio. Los resultados de DFT indican que el compuesto de silicio tetracoordinado es una molécula estable (punto de mínima energía) mientras que la especie hexacoordinada es un punto silla de primer orden (estado de transición). Los resultados teóricos son consistentes con los hallazgos experimentales y permiten racionalizar estos últimos.
**Palabras clave**: Silicio, dietilenglicol, hipervalencia, cálculos de funcionales de la densidad, función de Fukui.

## Introduction

Nowadays, silicon chemistry has gained great importance in the development of new polymers, glasses and ceramics [1]. Alkoxysilanes have proved to be suitable sources for the preparation of silica of different kinds (colloidal, nanoparticles or gels) as well as several types of hybrid copolymers with polyurethanes, polyesters, polyacrylates, etc. [2]. In particular, tetraethylorthosilicate (TEOS) and tetramethylorthosilicate (TMOS) are the main sources in the preparation of some materials through the sol-gel process. Some achievements in this field are the production of lamellar silica [3] through hydrolysis control using neutral diamine or the preparation of hybrid materials that involve fullerenes [4] or macromonomers [5].

There is great variety of homo- and heteroleptic tetraalkoxysilanes, most of them commercially available and there are several reports on silicon homoleptic, neutral and anionic complexes with aliphatic diols where the silicon atom is tetra- or hyper-coordinated [1c,6]. Recent studies have demonstrated the stability of Si – O – C linkages towards hydrolysis in the case of hypercoordinated silicon complexes [7]. These types of alkoxysilanes open different routes to the preparation of useful silanes or new materials [8]. This has stimulated our interest to study the formation of alkoxysilanes with aliphatic diols that are potentially able to act as tridentate dianionic ligands to yield homoleptic, hypercoordinated, and neutral alkoxysilanes.

Given the previous information, we studied the behaviour of diethyleneglycol, $O(CH_2CH_2OH)_2$, as a ligand towards a silicon centre. Several years ago it was reported that the reaction between diethyleneglycol and $SiCl_4$ yields an air-unstable bis-chelate tetracoordinated complex [6d,e] but a complete charac-

terization of this compound was not fully reported and any description on the other products obtained in this reaction was not discussed; particularly, no evidence with respect to the coordination number of silicon for the products has been presented so far. Nevertheless, some heteroleptic organosilicon complexes of diethyleneglycol of the type [RR'Si(dieng)] (dieng = diethyleneglycolate dianion) have been reported [9]. While some of these studies establish that this ligand acts as a bidentate, dianionic donor [9a-c], others suggest a tridentate coordination towards silicon [9d], but it has been reported that in the compound [Me$_2$Si(dieng)] $^{29}$Si NMR showed an absence of O – Si interaction [9b]. In fact, there is a lack of crystallographic data, theoretical calculations or spectroscopic evidence in order to support several of these proposals. On the other hand, it is well known that diethanolamine and their N-substituted derivatives (O,N,O-donor ligands, structural analogous of diethyleneglycol) act very often as tridentate ligands towards silicon [10]. It has been established that the presence of R bulky groups on the nitrogen atom avoids its coordination to the silicon atom both for steric and electronic reasons. Accordingly, from the great silicon-oxygen affinity as well as the interaction of the silicon atom with several (four) alcoxy fragments (electron-withdrawing ligands) it should be expected [1a,11-13] that the neutral complex bis(diethyleneglycolate)silicon(IV) will be hexacoordinated (A, scheme 1). Corriu has reviewed the hypervalent complexes of silicon [12] stating that neutral compounds can be formed from tetracovalent molecules by coordination of uncharged donors of groups 15 and 16, particularly when there is more than one electronegative ligand bonded to the parent silicon compound. This situation is illustrated by the crystalline hexavalent complex [Si(cat)$_2$(THF)$_2$] (cat = catecholate dianion) that, in addition to the 4-phenoxy donor moieties, contains the neutral O-donor ligand THF [14] (B, scheme 1). This is a coordinating framework analogous to that of structure A of scheme 1.

Similarly, intramolecular coordination from a donor group is aided by the rigid geometry of the ligand in which the donor atom is always held in close proximity of the Si centre. This is also possible with ligands for which there exist a favourable conformation allowing interaction between the silicon and the donor atom [12]. All these requirements seem to be fulfilled
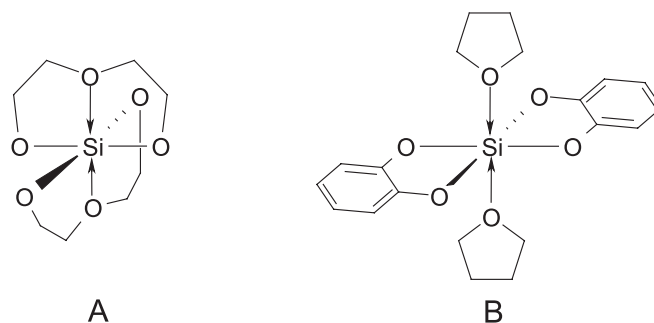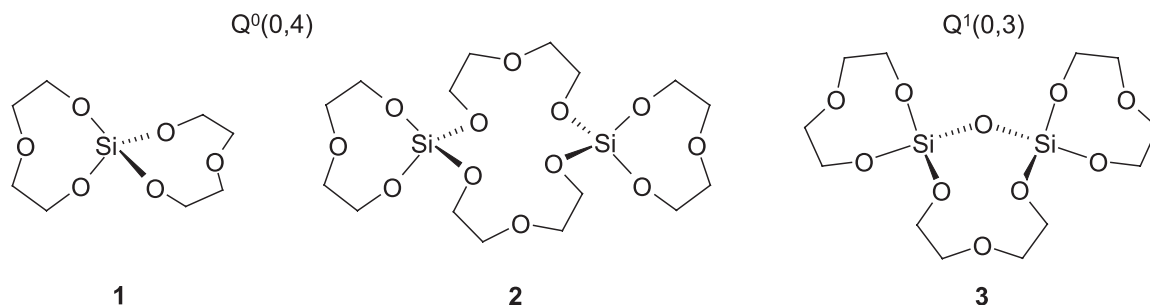


**Scheme 1**

by the ligand diethyleneglycolate; nevertheless, we were only able to prepare, isolate and fully characterize a spirocyclic tetracoordinated silicon complex (**1**, scheme 2). We also detected spectroscopically the formation of other oligomeric species of silicon with deprotonated diethyleneglycol (**2** and **3**, scheme 2), but as in the previous case, in these complexes the silicon atom is tetracoordinated and no evidence of formation of any hypervalent alkoxysilane was observed.

Density Functional Theory (DFT) calculations [15] at the BP86/TZ2P level of theory/numerical precision were performed to rationalize why diethyleneglycol apparently acts only as a dianionic, bidentate ligand towards silicon. We find from the harmonic frequencies analysis that the tetracoordinated complex structure is an energy minimum (stable molecule) whereas the hexacoordinated species is a transition state. DFT reactivity descriptors such as the Fukui condensed functions [16] were also evaluated and their usefulness to understand the observed reactivity and relative stabilities are discussed.

## Experimental

**General Methods**. All reactions and manipulations were carried out using standard Schlenk techniques under dried ultra-high purity N$_2$ (Infra, 99.999%) used as the inert gas. Methylene chloride (CH$_2$Cl$_2$) was dried and distilled from



**Scheme 2**

$P_2O_5$. Hexanes were refluxed and distilled from NaH. Diethyleneglycol 99.5% (Aldrich) was dried and distilled from metallic sodium. Silicon tetrachloride ($SiCl_4$) 99%, triethylamine 99.5%, and deuterated chloroform ($CDCl_3$) 99.9% were purchased from Aldrich and were used as received, by manipulating them under $N_2$. $^1$H, $^{13}$C, and $^{29}$Si NMR spectra were recorded on Gemini 200 MHz ($^1$H and $^{13}$C) and Varian Unity-Plus 300 MHz (multinuclear) spectrometers in $CDCl_3$ solutions. Chemical shifts (δ) are referenced to tetramethylsilane (TMS) at 0 ppm in all cases. IR spectra were recorded on an FT-IR Perkin-Elmer 1600 spectrometer. The mass spectra were determined by GC-MS analysis in a CP-3800 Gas Chromatograph coupled to a Varian Saturn 2000 Mass Spectrometer (electronic impact); detection interval: 40-650 *m/z*. The gas chromatograph was equipped with a capillary column Varian Chrompack CP-SIL 8 CB Low bleed /MS. 30 m x 0.25 mm ID, DF = 0.25 microns, and an ion trap detector using helium as the transporting gas (1 mL/min). Elemental analysis was performed with a Thermo-Finnigan Flash 1112 instrument. X-ray crystallographic data were collected in an Enraf-Nonius Kappa diffractometer with CCD area detector using graphite-monocromated Mo-K$_a$ radiation (l = 0.71073 Å) at 293(2)°K; data collection parameters and structure refinement details are summarized in table 1.

**Synthesis of 1,** Si[(OCH$_2$CH$_2$)$_2$O]$_2$: 1,4,7,9,12,15-Hexaoxa-8-silaspiro[7.7]pentadecane (8CI,9CI). In a Schlenk flask, 0.035 mol of diethyleneglycol were dissolved with 50 mL of $CH_2Cl_2$ and 0.07 mol (10 mL) of triethylamine. A solution of 0.018 mol of $SiCl_4$ in 50 mL of $CH_2Cl_2$ was slowly added to the diethyleneglycol/triethylamine solution at – 80°C with continuous stirring. The cold bath was allowed to warm at room temperature for about 3 h. The solvent was evaporated in the vacuum line and the white solid was extracted with 30 mL of hexanes. The solution was concentrated to 15 mL and stored overnight at 5°C yielding a colourless crystalline solid that corresponds to Si[(OCH$_2$CH$_2$)$_2$O]$_2$, **1**; yield 10%. The crystals are air-stable. A similar reaction was accomplished avoiding the addition of triethylamine yielding an oily colourless liquid when the $CH_2Cl_2$ was evaporated. This product contains the spirocyclic compound **1** together with dimers **2** and **3** (scheme 2). Physical and spectrometric data for **1**: Mp 79-80 °C. IR (KBr): 2942, 2879 cm$^{-1}$ C – H ; 1116 cm$^{-1}$ Si – O – C; 923 cm$^{-1}$ Si – O. $^1$H NMR (200 MHz, $CDCl_3$, 25 °C): δ 3.97 (m, 4 H, C$H_2$ – O – Si), δ = 3.71 (m, 4 H, C$H_2$ – O – C$H_2$), $^{13}$C NMR (50.28 MHz, $CDCl_3$, 25 °C): δ = 72.1 (*C*$H_2$ – O – Si), δ = 63.9 (*C*$H_2$ – O – *C*$H_2$). $^{29}$Si NMR (59.59 MHz, $CDCl_3$, 25 °C): δ = –81.5 (CH$_2$ – O – *Si*). GC-MS: Ret. time 10 min, *m/z* = 236 [M]$^+$. Anal. Calcd. for $C_8H_{16}O_6Si$: C, 40.66; H, 6.82. Found: C, 40.70; H, 7.01.

## Theoretical Methodology

All DFT calculations reported in this work were performed with the ADF v. 2003 program [17]. A local density approxi-

mation (LDA) functional based on the Vosko, Wilk and Nusair (VWN) functional [18] combined with the Becke's exchange [19] and Perdew's correlation [20] (BP86) non-local corrections, were self-consistently employed. We chose the best basis sets by optimizing the diethyleneglycol ligand geometry, using Slater-type-orbital (STO) functions with single-, double- and triple-z quality. All-electron and polarized functions, in the second and third cases, were used for the best compromise between computational cost and the observed minor deviations on the ligand structure parameters. The final calculations are all reported at the BP86/TZ2P level of theory/numerical precision. The frontier molecular orbitals were generated and visualized with the MOLEKEL program [21]. Isotropic shell calculations and derived chemical shifts with respect to TMS were computed with a program [22] from Ziegler's group for the calculation on the ADF output file. Harmonic vibrational frequencies were calculated to verify the stationary points found for all species, according to the discussion in section III, adding the zero-point energy correction to the calculated functional energy. By means of the so-called condensed Fukui functions [16] computed at the Si and O atoms, we obtain quantitative reactivity parameters for these complexes.

## Results and Discussion

### 1. Experimental Results

The reaction of $SiCl_4$ and diethyleneglycol in the absence of triethylamine yields a mixture of three products as revealed by $^{29}$Si NMR (see Figure 1). To design the different silicon compounds, the Q$^n$(*i,j*) notation was used (Scheme 2): Q represents the SiO$_4$ moiety and *n*, *i* and *j* are the substituents on oxygen atoms: SiO$_3$, H and R (alkyl), respectively. [2c] There are two signals at δ – 81.5 and – 82.1 ppm in an approximate ratio 2:1
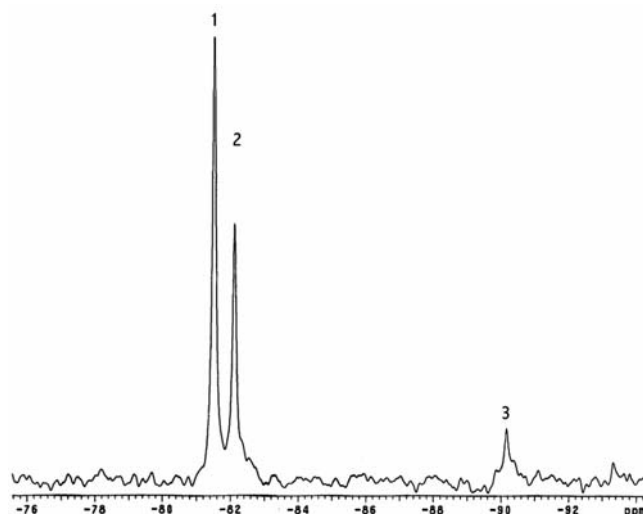


**Fig. 1.** $^{29}$Si NMR spectrum in $CDCl_3$ of the crude of the reaction $SiCl_4$/diethyleneglycol without triethylamine.

that correspond to two different tetraalkoxysilane $Q^0(0,4)$ species, **1** and another that could be an oligomer with a structure like **2**, respectively (see Scheme 2). There is a third weaker signal at – 90.2 ppm that corresponds to a $Q^1(0,3)$ silicon species that should be the hexa-alkoxy-disiloxane complex **3** [2c,23]. Any penta- or hexacoordinated species of silicon with this ligand must absorb up-field in the region from about –110 to –150 ppm [13,24] but no signals were detected in this zone.

$^1$H NMR spectrum of the crude of the reaction without triethylamine shows two sets of complex multiplets centred at 3.98 and 3.66 ppm, while $^{13}$C NMR spectra show several signals in the range between 62 and 72 ppm.

Due to its greater solubility in hexanes, it was possible to separate the fraction that gives rise to the stronger signals in $^{29}$Si NMR (compound **1**, *vide infra*) together with some impurities. However it was more convenient to transform the mixture of compounds to the thermodynamic product (**1**) by refluxing the crude of reaction in $CH_2Cl_2$ over a period of 3 days. Subsequently, $^1$H NMR spectrum becomes quite simple showing two symmetric multiplets centred at 3.90 and 3.64 ppm typical of an AA'BB' Z – $CH_2$ – $CH_2$ – Y system [25a]. The $^{29}$Si NMR signal of this product corresponds to the main signal in the crude of reaction, **1**. Although in low yield, a pure sample of **1** was obtained by the method described in the experimental section, where the reaction is accomplished with the presence of triethylamine for neutralize the HCl formed during the reaction. The $^1$H, $^{13}$C and $^{29}$Si NMR data for this sample are consistent with the results for compound **1** already shown.

In order to support the proposal for the three structures shown in Scheme 2 and the corresponding assignments in $^1$H and $^{29}$Si NMR, the crude of the reaction without triethylamine was analyzed by gas chromatography – mass spectrometry. The chromatogram shows only two fractions, at retention times of 10 and 18 minutes. The fraction that appears after 10 minutes shows the heavier peak in mass spectrometry with an $m/z = 236$ (48%) and the isotopic pattern of $C_8H_{16}O_6Si$ that corresponds to the molecular ion of **1**. There is a peak that corresponds to the fragment [$M^+ - C_2H_4O$] ($m/z = 192$, 30%) and concomitantly the fragment [$C_2H_4O$]$^+$ ($m/z = 44$, 30%) is present; cleavage of the bond C – C next to the oxygen atom in alcohols (alkoxyde, in the present case) is of general occurrence in mass spectrometry [25b]. On the other hand, the chromatographic fraction with a retention time of 18 minutes shows a heavier peak at $m/z = 384$ that is very weak (5% abundance) but reveals a residual isotopic peak [$M^+ + 1$] that suggests the formula $C_{12}H_{24}O_{10}Si_2$ corresponding to compound **3**. Nevertheless, three fragments that correspond to the species [$M^+ - C_2H_4O$] ($m/z = 340$, 12%), [$M^+ - C_4H_8O_2$] ($m/z = 296$, 77%) and [$M^+ - C_6H_{12}O_3$] ($m/z = 252$, 80%) with the right isotopic patterns are present. The fragment [$C_2H_4O$]$^+$ ($m/z = 44$, 15%) is also present. What could be the dimer **2** was not detected by this method, probably due to its instability in the gas chromatography conditions as a consequence of its great molecular weight (472 g/mol). It is also probable that during the GC-MS process, it transforms into the monomer **1**, as it

happens when it is refluxed in $CH_2Cl_2$ for three days (*vide supra*). Our proposal of structure **2** for the signal at – 82.1 ppm in $^{29}$Si NMR is mainly due to the fact that we are not aware of other possibilities for a $Q^0(0,4)$ complex with this ligand that would be soluble in $CH_2Cl_2$ and hexanes and able of transforming almost cleanly to complex **1** simply by refluxing in $CH_2Cl_2$. On the other hand, formation of dimer **3** can be a consequence of the great oxophilia of the silicon atom, leading to cleavage of some C – O bonds of diethyleneglycol. In fact, there appear some organic by-products that give $^1$H and $^{13}$C NMR signals corresponding to olefinic species.

## 2. X-Ray Crystal Structure of 1.

A single crystal of compound **1** obtained as described in the experimental section was mounted on a glass fibber. Structure solution and refinement were carried out using SHELX-97 [26] included in the package Wingx [27]. The structure was solved by direct methods and all non-hydrogen atoms were refined anisotropically. Hydrogen atoms were placed at idealized positions. Crystal data, data collection parameters and structure refinement details are summarized in Table 1.

**Table 1:** Crystal and Structure Refinement data for compound **1**.

| | |
|---|---|
| Empirical formula | $C_8H_{16}O_6Si$ |
| Formula mass [g mol$^{-1}$] | 236.30 |
| Temperature [K] | 293(2) |
| Crystal size [mm] | 0.6 x 0.25 x 0.25 |
| Crystal descript | Colourless prism |
| Crystal system | Orthorhombic |
| Space group | $P\ 21\ 21\ 21$ |
| $a$ [Å] | 9.2892(3) |
| $b$ [Å] | 9.5845(3) |
| $c$ [Å] | 12.3748(4) |
| $\alpha$ [°] | 90.00 |
| $\beta$ [°] | 90.00 |
| $\gamma$ [°] | 90.00 |
| $V$ [Å$^3$] | 1101.76(6) |
| Z | 4 |
| $r_{calc}$ [g cm$^{-3}$] | 1.425 |
| $\mu$ [mm$^{-1}$] | 0.220 |
| $F(000)$ | 504 |
| $2\theta$ range [°] | 8.50-50.58 |
| Index ranges | $-10 \le h \le 8$ |
| | $-9 \le k \le 11$ |
| | $-14 \le l \le 14$ |
| No. of collected reflcns | 7158 |
| No. of observed reflcns | 1690 |
| Reflcns unique | 1896 ($R_{int}$ = 0.0315) |
| $R1^a$, $wR2^a$ (2s data) | 0.0390, 0.0827 |
| $R1^a$, $wR2^a$ (all data) | 0.0477, 0.0883 |
| Max/min transm | 0.8649/0.7434 |
| Data/restr/params | 1896/0/137 |
| GOF on $F^2$ | 1.049 |
| Larg diff peak/hole [eÅ$^{-3}$] | 0.272/-0.225 |

$^a R1 = \Sigma||F_o| - |F_c||/\Sigma|F_o|$; $wR2 = [\Sigma w(F_o - F_c)2/\Sigma wF_o^2]^{1/2}$ are given for observed data.
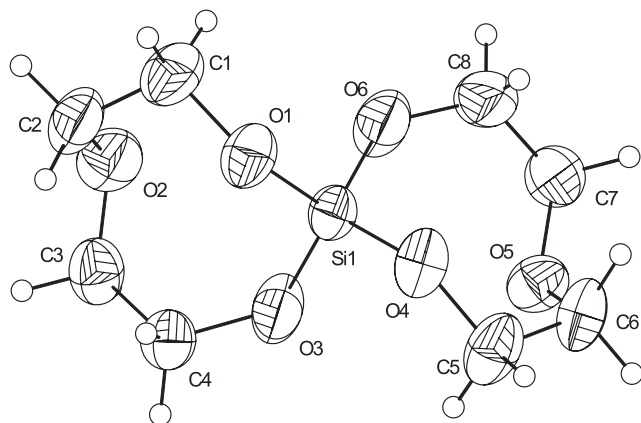
**Fig. 2.** Crystal structure of **1** with anisotropic displacement parameters depicting 50% probability.

Figure 2 shows the ORTEP representation of the crystal structure of compound **1,** depicting 50% probability. Selected bond distances and angles are reported in Table 2. Figure 2 shows a tetracoordinated silicon with typical alkoxysilane Si – O bond lengths [28] (1.610 to 1616 Å); however, it is important to notice that non-bonded Si – O(2) and Si – O(5) distances (3.144 and 3.063 Å, respectively) even larger for a Si – O covalent bonding (1.66 Å), are smaller than the sum of the van der Waals radii of Si and O atoms (3.60 Å) [29]. This suggests some long-distance interactions similar to those of silicon – diethanolamine complexes when the nitrogen atom carries a bulky group [10]. These plausible weak interactions in **1** are presumed from deformation of the tetrahedral polyhedron of silicon: only three of the O – Si – O angles of the SiO₄ moi-

ety are close to the ideal value of 109.5°, but there are two bigger angles (around 112.5°) and a smaller one (closer to 103°, see Table 2).

A low basicity for ethereal, uncoordinated oxygens is revealed by the angles formed by these atoms and their adjacent carbon atoms: C(3) – O(2) – C(2) and C(6) – O(5) – C(7) angles (116.4 and 117.3, respectively) are relatively open as to consider that the lone electron pairs on the oxygen atoms have a low p-character; as comparison, the C – O – C angles of coordinated THF molecules in the complex [Si(cat)₂(THF)₂] (B scheme 1) has a value of 110.5° [14] corresponding to a bigger p-character for the lone electron pairs on the coordinated oxygen. The angles values for C(3) – O(2) – C(2) and C(6) – O(5) – C(7) fragments of complex **1** are in good agreement with those obtained by means of the theoretical calculations (Table 3; *vide infra*).

## 3. Theoretical Results

### Free diethyleneglycol ligand calculation and Basis Set Selection.

Optimised geometrical parameters of diethyleneglycol, obtained with different basis sets, are shown in Figure 3 and Table 3. According to these results, bond lengths in the ligand are shortened as the numerical basis increases in size and there are similar results between the DZP and TZ2P basis sets. Poorer results are obtained for the BP86/SZ calculations [18], although the BP86/DZP and BP86/TZ2P structures including d-type polarization functions for carbon and oxygen atoms and p-type polarization functions for hydrogen (latter basis set) provide smaller deviations in the ligand bond lengths. A

**Table 2:** Selected bond lengths [Å] and angles [°] for compound **1**.

| | | | |
|---|---|---|---|
| C(1) – O(1) | 1.433(4) | C(1) – C(2) | 1.499(5) |
| C(2) – O(2) | 1.426(4) | C(3) – O(2) | 1.416(4) |
| C(3) – C(4) | 1.489(4) | C(4) – O(3) | 1.417(4) |
| C(5) – O(4) | 1.425(4) | C(5) – C(6) | 1.485(5) |
| C(6) – O(5) | 1.411(4) | C(7) – O(5) | 1.416(4) |
| C(7) – C(8) | 1.430(5) | C(8) – O(6) | 1.353(4) |
| Si – O(1) | 1.612(2) | Si – O(3) | 1.615(2) |
| Si – O(4) | 1.614(2) | Si – O(6) | 1.610(2) |
| Si – O(2) | 3.144 | Si – O(5) | 3.063 |
| | | | |
| O(1) – C(1) – C(2) | 111.9(3) | O(2) – C(2) – C(1) | 109.2(3) |
| O(2) – C(3) – C(4) | 113.1(3) | O(3) – C(4) – C(3) | 111.7(3) |
| O(4) – C(5) – C(6) | 112.6(3) | O(5) – C(6) – C(5) | 109.1(3) |
| O(5) – C(7) – C(8) | 114.0(3) | O(6) – C(8) – C(7) | 120.7(3) |
| C(1) – O(1) – Si(1) | 125.9(2) | C(3) – O(2) – C(2) | 116.4(3) |
| C(4) – O(3) – Si(1) | 124.1(2) | C(5) – O(4) – Si(1) | 125.88(19) |
| C(6) – O(5) – C(7) | 117.3(3) | C(8) – O(6) – Si(1) | 129.3(2) |
| O(6) – Si(1) – O(1) | 109.39(13) | O(6) – Si(1) – O(3) | 109.79(15) |
| O(1) – Si(1) – O(3) | 112.18(12) | O(6) – Si(1) – O(4) | 112.97(13) |
| O(1) – Si(1) – O(4) | 102.87(12) | O(3) – Si(1) – O(4) | 109.53(12) |

slight decrease in the C – C bond in the last two basis-set calculations is observed. The difference between calculated bond distances is less than 0.008 Å, in BP86/DZP and BP86/TZ2P. Therefore, the choice of either DZP or TZ2P basis sets does not vary the optimized ligand geometry considerably. However, since the larger basis set may account more for the finer details in the wavefunction-derived properties and the CPU computing time to calculate the optimized BP86/DZ and BP86/TZ2P structures is not dramatically different, we decided to use the TZ2P basis set in the next calculations of the silicon complexes. Therefore, our reported results for the complexes are all at the BP86/TZ2P level of theory/numerical precision.

By examining the isolated ligand with the previous selected level of theory, we computed the electronic properties showed in Figure 3 and the Highest Occupied Molecular Orbital (HOMO) and Lowest Unoccupied Molecular Orbital (LUMO) displayed in Figure 4. These properties will be discussed in the next sections of the silicon complexes. For now, let us notice the highest absolute values of Voronoi-type charges are on the future coordinated oxygens, according to the trend pointed out by the HOMO of this molecule. Nucleophilic condensed Fukui values predict the reactive sites at the hydrogens to be substituted (1 and 1' labels) as expected (having the highest values: -0.235, respect to the other atoms). Also, electrophilic condensed Fukui values are larger on the oxygens atoms: -0.235 (for 21 and 23 labels) and -0.177 (for 22 label), as it can be seen in Figure 3. As these values go in the same direction as the Voronoi-type charges (the negative sign indicates more charge to be donated), we can say we have identified the reactive sites on this ligand. The most electron donors atoms are the hydroxilic atoms followed by the ethereal oxygen, which has good donor capacity but less than the first ones.

## Tetrahedral Complex

In Table 4, we present the more relevant geometrical parameters of the calculated tetrahedral silicon compound (Figure 5); geometrical structure nicely agrees with the X-ray data (compare with Table 2). Diethyleneglycol ligands are perpendicular to each other. We found that bond lengths and angles of oxygen-silicon bonds are the same in both ligands, just like the rest of the bonding lengths and angles. Furthermore, in accordance with the experimental results (see Table 2), the computational results revealed that the Si – O(1) bond (1.632 Å) is slightly shorter than the Si – O(3) bond (1.653 Å) and similarly with the Si –O(6) and Si – O(4) bonds respectively, reflecting the relative *trans* effect between the two ligands with same chemical environment. The effect in the oxygen atoms in the complex leads to the relative elongation on some C – O bonds as can be noted in the difference of 0.008 Å between C(6) and C(7) linked to the same O(5) atom since the electron lone pairs in the oxygen atoms promote a different density around carbon nuclei. Harmonic frequencies analysis of this structure shows this stationary point is a true energy minimum.
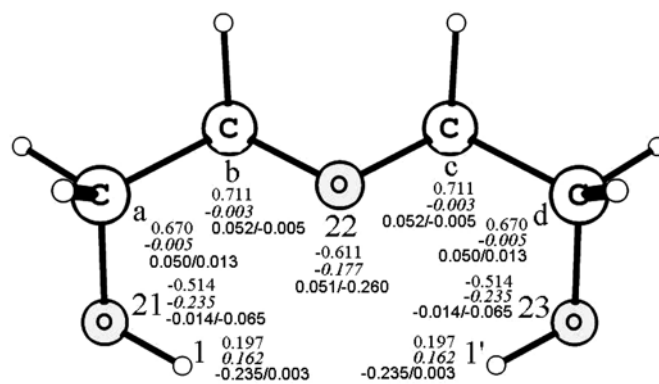


**Fig. 3.** Optimized geometries for diethyleneglycol ligand at (a) BP86/SZ, (b) BP86/DZP and (c) BP86/TZ2P level of theory. See Table 3 for numerical values. Mulliken derived-charges, Voronoi deformation density charges in italics and condensed nucleophilic/electrophilic Fukui functions are shown respectively besides each atom calculated at BP86/TZ2P level.

**Table 3.** Representative bond lengths (Å) of diethyleneglycol ligand at BP86 level of theory with different basis sets. See Figure 3 for the labels on each atom.

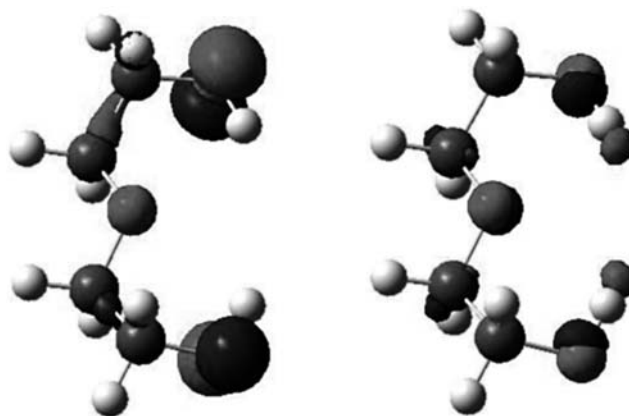| Bond | BP86/SZ | BP86/DZP | BP86/TZ2P |
|---|---|---|---|
| Ca – Cb | 1.579 | 1.511 | 1.518 |
| Cc – Cd | 1.579 | 1.511 | 1.518 |
| Cb – O(22) | 1.481 | 1.433 | 1.430 |
| Cc – O(22) | 1.481 | 1.433 | 1.430 |
| O(21) – H(1) | 1.040 | 0.978 | 0.974 |
| O(23) – H(1') | 1.040 | 0.978 | 0.974 |



**Fig. 4**. Frontier Molecular Orbitals of the diethyleneglycol ligand are illustrated: HOMO (left) and LUMO (right).

**Table 4.** Bond lengths (Å) and angles (°) calculated for tetrahedral (Figure 5) and pseudo-octahedral (Figure 7) structures of silicon bis-diethyleneglycol complex at BP86/TZ2P level of theory.

| Bond length | Tetrahedral Complex | Pseudo-octahedral Complex |
|---|---|---|
| Si – O(1) | 1.632 | 1.632 |
| Si – O(3) | 1.653 | 1.645 |
| Si – O(4) | 1.653 | 1.654 |
| Si – O(6) | 1.632 | 1.627 |
| Si – O(2) | 3.335 | 3.474 |
| Si – O(5) | 3.335 | 3.655 |
| C(1) – O(1) | 1.421 | 1.421 |
| C(2) – O(2) | 1.433 | 1.430 |
| C(3) – O(2) | 1.432 | 1.431 |
| C(4) –O(3) | 1.422 | 1.432 |
| C(5) – O(4) | 1.422 | 1.425 |
| C(8) – O(6) | 1.421 | 1.421 |
| C(6) – O(5) | 1.425 | 1.425 |
| C(7) – O(5) | 1.433 | 1.428 |
| | | |
| **Bond angle** | | |
| | | |
| O(1) – Si – O(3) | 115.3 | 112.6 |
| C(4) – O(3) – Si | 132.0 | 130.4 |
| C(1) – O(1) – Si | 133.8 | 134.2 |
| C(3) – O(2) – C(2) | 117.4 | 118.2 |
| O(4) – Si – O(6) | 115.3 | 113.1 |
| Si – O(4) – C(5) | 133.8 | 132.2 |
| Si – O(6) – C(8) | 132.0 | 135.6 |
| C(6) – O(5) – C(7) | 117.3 | 118.0 |
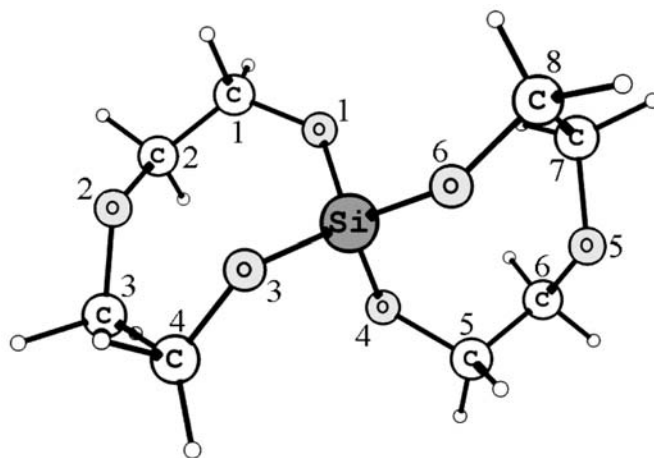


**Fig. 5.** Coordination mode and labelling of tetrahedral silicon bis-diethyleneglycol complex. See Table 4 for numerical values.

In Figure 6, the HOMO and LUMO (frontier orbitals of this complex) are shown. From a chemical point of view, the sites with highest absolute values of the HOMO represents the region where the molecule more easily donates electronic charge, acting there like a nucleophilic agent and the sites with highest absolute values of the LUMO depicts the regions where the molecule more readily accepts electronic charge, thus acting there like an electrophilic agent. For major clarity, we have mapped the absolute value of the HOMO of the com-
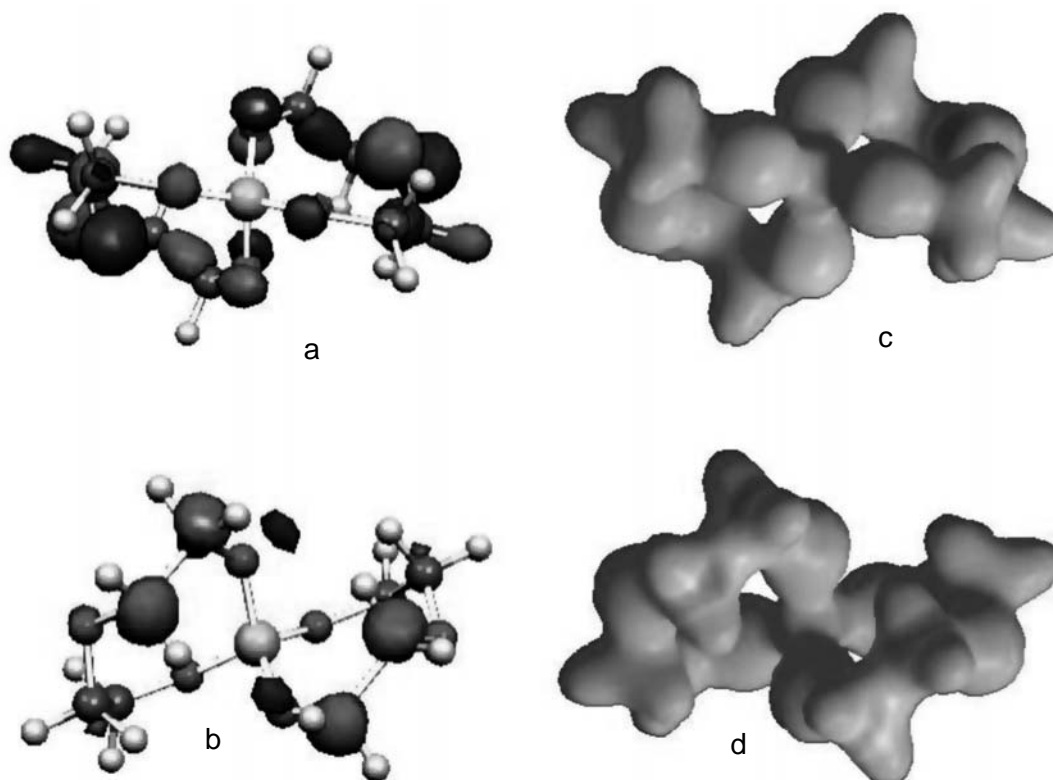


**Fig. 6.** Frontier Molecular Orbitals and density maps of the tetrahedral silicon complex are illustrated. a) HOMO; b) LUMO; c) HOMO mapped onto 0.08 a.u. density isosurface and d) LUMO mapped onto 0.08 a.u. density isosurface.

plex onto a 0.08 a.u. density isosurface, and observe the HOMO behaviour closer to the nuclei (see Figure 6). One can see the highest values (blue) in two regions (it is delocalized allowing a minor regioselectivity to carry out a reaction) but there is clearly a notable difference between the O(2) and O(5) atoms. In the first, the blue (higher absolute value) of the HOMO is pointing outside from the complex whereas in the second, the HOMO is pointing towards silicon directly. This indicates different coordination behaviour of these two oxygen atoms towards the silicon centre.

The different reactivity of each symmetric pair of oxygen atoms has been corroborated through inspection of the Voronoi Deformed Density (VDD) derived charges [30], listed in Table 5, which are defined as the integrated difference between the electron density on each atomic basin in the molecule minus the electron density of the isolated atom. This atom-in-molecule charge-like parameter reveals a trend to donate electrons in the following order: O(2)/O(5) >> O(1)/O(6) > O(3)/O(4), which is in good agreement with the interpretation discussed above of the HOMO map; also provides an additional indication for the experimental synthesis of bis-chelate complex suggesting the possibility of forming a coordination bond between one of the free oxygen atoms and the silicon atom.

We have carried out one more calculation to further support our analysis of the different O-donating abilities in the complexes. By means of the DFT [15] so-called Fukui functions [31] [f($\mathbf{r}$)], we may quantitatively establish the difference of reactivity in the free oxygen atoms or those bound to the Si centre. These indexes measure the change of chemical potential (m) of the molecule with respect to the external potential [v($\mathbf{r}$)], imposed by the nuclei, due to any perturbation in the system at one point, and is expressed as

$$f(\bar{r}) = \left[ \frac{\delta \mu}{\delta v(\bar{r})} \right]_N = \left[ \frac{\partial \rho(\bar{r})}{\partial N} \right]_v \tag{1}$$

The second equality in eq. (1) follows from a Maxwell relation and is the response of the total electron density (r) of the atom or molecule with respect to a change in the total number of electrons (N) [15]. There is a discontinuity in this derivative since it only takes discrete values in processes where an entire electron is lost (N-1) or won (N+1). This is, in common practice, evaluated by finite-difference methods, assuming that the electron density undergoes small changes and thereby we obtain, depending on the process, either a nucleophilic $f^+($r$)$ or electrophilic $f^-($r$)$ Fukui function, useful to assess site reactivity towards these kind of attacks, that may be respectively approximated by the HOMO and LUMO densities, assuming that there is no orbital relaxation (unrelaxed approximation) [15,31].

$$f^+(\bar{r}) \approx r(N+1) - r(N) \cong r_{LUMO}(\bar{r})$$
$$f^-(\bar{r}) \approx r(N) - r(N-1) \cong r_{HOMO}(\bar{r}) \tag{2}$$

We can integrate this quantity around each atomic basin within the molecule so that we may describe reactivity in a specific atom. These are the corresponding condensed Fukui functions [16], which are defined analogously to eq. (2) but now in terms of atomic charges $q$ at the $k$-atom

$$f_k^+ = q_k(N+1) - q_k(N)$$
$$f_k^- = q_k(N) - q_k(N-1) \tag{3}$$

We evaluated the condensed Fukui functions by means of eq. (3), using Mulliken atomic charges, which are reported in table 6. As can be observed, the behaviour of the oxygen atoms in the tetrahedral complex follows the same trends as the VDD charges for a nucleophilic attack (when it coordinates to the Si centre). This is in complete accord with what was already discussed above with other reactivity descriptors.

Furthermore, we carried out calculations of the chemical shifts (from the computed total isotropic NMR shieldings with respect to the computed TMS value) over the protons and the silicon centre of the studied system. Results are shown in Table 7. In general all values are in agreement with the experi-

**Table 5**. Voronoi deformation density charges computed at the BP86/TZ2P level of theory/numerical precision located at the oxygen and silicon atoms in the tetrahedral and octahedral compounds of silicon complex.

| Atom | Tetrahedral complex | Pseudo-Octahedral complex |
|---|---|---|
| Si | 0.458 | 0.452 |
| O(4) | -0.246 | -0.260 |
| O(3) | -0.246 | -0.252 |
| O(6) | -0.233 | -0.232 |
| O(1) | -0.233 | -0.240 |
| O(2) | -0.159 | -0.170 |
| O(5) | -0.159 | -0.172 |

**Table 6.** Condensed Fukui functions calculated from Mulliken atomic charges at the BP86/TZ2P level of theory/numerical precision by using eq. (3) on the oxygen and silicon atoms for the tetrahedral and pseudo-octahedral Si complexes.

| Atom (i) | Tetrahedral complex | | Pseudo-Octahedral complex | |
|---|---|---|---|---|
| | $f_i^+$ | $f_i^-$ | $f_i^+$ | $f_i^-$ |
| Si | 0.0766 | -0.0105 | 0.0982 | -0.0230 |
| O(4) | -0.0098 | -0.0474 | -0.0063 | -0.0707 |
| O(3) | -0.0098 | -0.0474 | -0.0053 | -0.0737 |
| O(6) | -0.0153 | -0.0435 | -0.017 | -0.0335 |
| O(1) | -0.0153 | -0.0435 | -0.0131 | -0.0764 |
| O(2) | 0.0061 | -0.0981 | 0.0094 | -0.0146 |
| O(5) | 0.0061 | -0.0981 | 0.0053 | -0.1142 |

**Table 7.** Theoretical chemical shifts at the BP86/TZ2P level of theory/numerical precision from total isotropic shieldings (ppm) calculated for protons and silicon atoms in the silicon bis-diethyleneglycol tetrahedral and pseudo-octahedral compounds (referenced to the computed TMS value). For atoms labels see Figs. 5 and 7.

| Atom(s) | Tetrahedral complex | Atom(s) | Pseudo-octahedral Complex |
|---|---|---|---|
| Si | 101.834 | Si | 101.266 |
| H(7B), H(2B) | 3.724 | H(7B) | 3.753 |
| H(7A), H(2A) | 3.833 | H(7A) | 3.563 |
| H(8B), H(1B) | 4.006 | H(8B) | 3.884 |
| H(8A), H(1A) | 3.547 | H(8A) | 3.727 |
| H(6B) | 3.802 | H(6B) | 3.804 |
| H(6A) | 3.697 | H(6A) | 3.314 |
| H(5B) | 4.069 | H(5B) | 4.065 |
| H(5A), H(4A) | 3.668 | H(5A) | 3.61 |
| H(3B) | 3.698 | H(1A) | 3.616 |
| H(3A) | 3.803 | H(1B) | 4.02 |
| H(4B) | 4.07 | H(2B) | 3.608 |
| | | H(2A) | 3.949 |
| | | H(3A) | 4.36 |
| | | H(3A) | 3.635 |
| | | H(4A) | 3.676 |
| | | H(4B) | 4.05 |

**Table 8.** More representative vibrational frequencies (cm$^{-1}$) calculated at the BP86/TZ2P level of theory for the silicon bis-diethyleneglycol tetrahedral and pseudo-octahedral compounds. Imaginary frequency was found to be 34.46*i*.

| Tetrahedral complex | Pseudo-Octahedral complex | Experimental |
|---|---|---|
| _735.08 | 728.34 | |
| 764.61 | 769.94 | |
| 909.52 | 924.77 | 923.0 |
| 994.44 | 990.26 | |
| 1139.37 | 1141.94 | 1116.0 |
| 1160.88 | 1161.65 | |
| 1265.09 | 1226.27 | |
| 1274.68 | 1280.31 | |
| 2944.19 | 2949.69 | 2879.0 |
| 2951.67 | 2956.47 | 2942.0 |
| 2961.47 | 2961.20 | |
| 2993.38 | 2997.57 | |
| 3004.70 | 3005.16 | |
| 3014.40 | 3017.46 | |

mental ones (see $^1$H NMR data for **1** in the experimental section for comparison).

The more intense vibrational frequencies of this complex are shown in Table 8. We found that the tetrahedral complex is a true energy minimum (only positive frequencies) on the potential energy surface (PES). In agreement with its observation and appropriate experimental characterization, the theoretical signals significantly correspond to the most important experimental ones. The characteristic value at 1160.88 cm$^{-1}$ contains the coordinated stretching mode of the C – O bonds and those at 909.52 cm$^{-1}$ are due to the Si – O bonds for stretching normal modes, confirming the interactions in the tetrahedral coordination that had been expected.

**Pseudo-Octahedral Complex**

Theoretical studies [32] analyzing the hexacoordinated behaviour of the silicon atom towards different atoms have been reported recently. To investigate why a similar hyper coordination apparently is not present in our synthesized molecule, we have carried out the geometry optimization of the pseudo-octahedral structure. Computed bonding distances and angles are reported in Table 4. Comparing total bonding relative energies we obtained that this complex (-6.4956 a.u.) is 4.39 Kcal/mol less stable (higher in energy) than the tetrahedral complex (-6.5026 a.u.). Subsequently we found from the harmonic frequencies analysis that the pseudo-octahedral complex is a first-order saddle point in the PES (one imaginary frequency, see Table 8) revealing its nature as a transition

state. This is meaningful for discarding the isolation of this complex and explains the experimental findings.

In Figure 6, the assumed pseudo-octahedral complex is depicted. *The final optimized geometry is similar to the tetrahedral complex* but the C$_s$ symmetry reflects some important geometrical parameters differing from the tetrahedral complex (see Table 4). By inspecting the complex geometry, it is shown that diethyleneglycol ligand conformations have only some similarities to those in the tetrahedral complex. Note that the Si – O(1) and Si – O(6) bond lengths are shorter than the Si – O(3) and Si –O(4), respectively, on the average by 0.025 Å, probably due to the *trans* effect. Nonetheless, this does not happen in the tetrahedral complex since the bonding angles
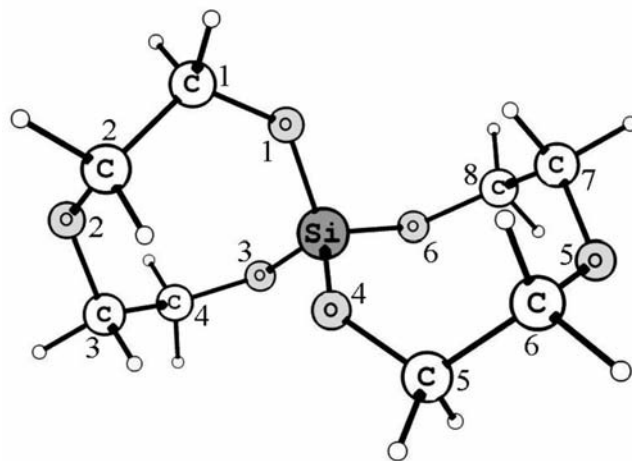


**Fig. 7.** Structure and labelling of pseudo-octahedral complex showing the coordination mode of this species. See Table 5 for the data on this compound.

between oxygen atoms and silicon are narrower and the C – O bond lengths in the free oxygen atoms are shortened leading to an unexpected stretching of Si– O(2) and Si – O(5) bonds.

Undoubtedly, this promotes an irregular tetrahedron and a non-symmetric charge distribution as we later discuss in detail. It is noted that whereas the optimized tetrahedral complex shows that the bonding lengths of O(2) and O(5) atoms remain at the same distance from the silicon atom (3.335 Å), in this octahedral case the O(2) atom is 0.18 Å closer to the silicon atom than O(5).

A more apparent difference is underscored by mapping the HOMO of the complex, as can be seen in Figure 8a. We can clearly observe that it is found almost totally over one of the ligands and precisely the largest concentration is on the oxygen O(2). Again, the highest (absolute) value in HOMO mapped onto a density isosurface (Figure 8c), directly points towards the Si centre. Also, the placement of the LUMO mapped onto a density isosurface is illustrated in Figure 8d, indicating the more electrophilic sites of the molecule can be compared with those of the totally tetrahedral species.

By analyzing the Voronoi deformation density derived charges, which are reported in Table 5, it can be seen that the loss of symmetry for this system creates different preferences towards the donating charge in all oxygen atoms of the pseudo-octahedral complex. More electrophilic is the O(5) atom, which is slightly more negative that its counterpart, the O(2) atom. This last is closer to silicon and delocalizes a larger region of

charge over the entire molecule. The unequal distribution of charge around the coordination sphere of silicon has slightly decreased its charge acceptor character as can be expected.

Calculated condensed Fukui functions for this complex are displayed in Table 6. The interpretation is that there is apparently a notable reactivity difference between the non-coordinated oxygen atoms towards the Si centre. The O(5) atom tends to accept more electronic charge than the O(2) atom (last column of Table 6) but the minor reactivity of the second is compensated by a major charge retrodonation of the silicon atom, which has increased its electron acceptance capacity with respect to the symmetric tetrahedral complex. Moreover, the O(2) atom has the highest positive nucleophilic Fukui value over the rest of the oxygen atoms and therefore it represents the species more capable of donating electronic charge over the entire molecule, according to the discussion of Figure 8.

Our theoretical results predict two conformers of different reactivity, in which one of them (lower in energy) can better interact with one of its free oxygen atoms towards the silicon centre, resulting in a major symmetry in the system that allows sharing electronic charges towards the Si centre. We may conclude that the complex, or more precisely, the position of the O-atoms around the Si atom is quite fluxional, reflecting the inherent conformational flexibility of the ligand and fluxionality of the overall system. We found that the higher energy conformer corresponds to a transition state with the reaction
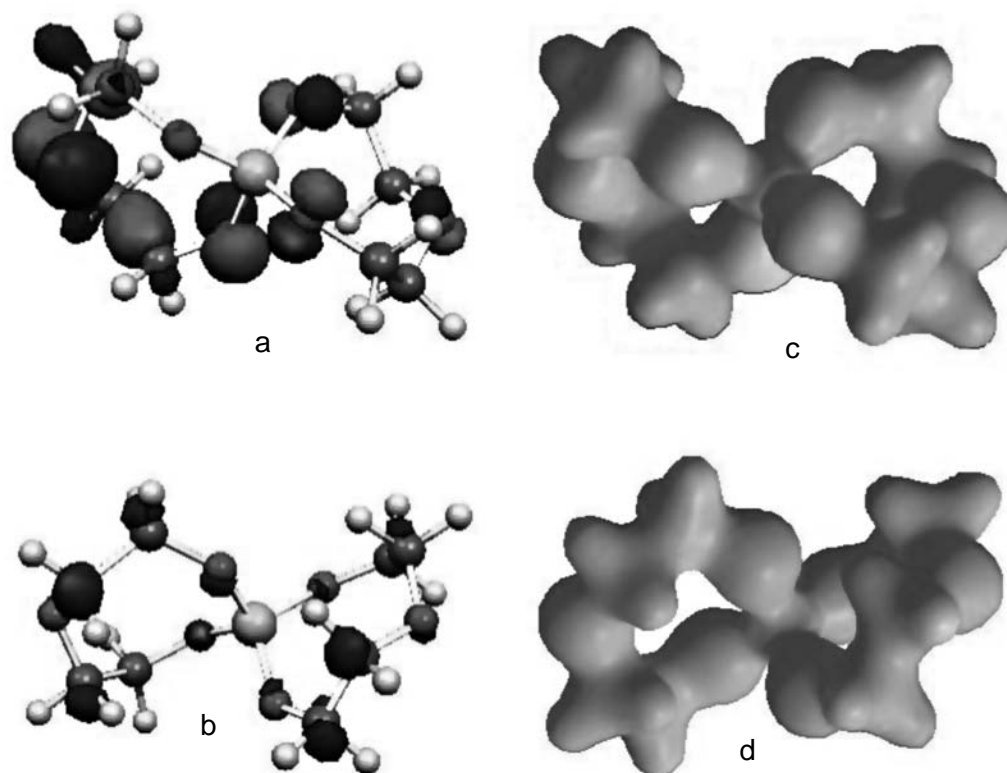


**Figure 8.** Frontier Molecular Orbitals and density maps of the pseudo-octahedral silicon complex are illustrated. a) HOMO; b) LUMO; c) HOMO mapped onto 0.08 a.u. density isosurface and d) LUMO mapped onto 0.08 a.u. density isosurface.

coordinate (at imaginary frequency 34.46*i*) corresponding precisely to the movement of O(2) outside of the chelate ring and increasing its distance from the metallic centre, followed by a rearrangement in the geometry of this ligand. Therefore, *the hexacoordinated silicon complex seems to be very improbable* but the theoretical analysis of the pseudo-octahedral structure can be seen as a possible way in postulating an isomerization mechanism from the tetrahedral complex. The mechanism could be an intramolecular movement passing through this transition state where it is plausible to donate an electronic charge from one of the ethereal oxygens, O(2), to the silicon centre whereas the other, O(5), tends to stretch its position. In Table 8, the more relevant calculated frequencies for the pseudo-octahedral species are also shown.

Finally, for the pseudo-octahedral complex we have also computed the chemical shifts (from the computed total isotropic NMR shieldings with respect to the computed TMS value) over the protons and the silicon centre of the complex. Results are shown in Table 7. In general all theoretical values are in agreement with what would be expected for this kind of complex. The theoretical values are somewhat different from the tetrahedral complex signals. This is expected, given the loss of symmetry in this non-stable pseudo-octahedral molecule (transition state).

## Conclusions

The ethereal oxygen in diethyleneglycol is apparently unable to coordinate with the silicon atom and this may be a consequence of the low basicity of this atom and no steric consideration needs to be accounted for as in the case of diethanolamine derivatives. As it was aforementioned, the low basicity of ethereal, uncoordinated oxygens is revealed by the angles formed by these atoms and their adjacent carbon atoms, that are in good agreement with those angles values obtained by means of the theoretical calculations (Tables 2 and 3). Moreover, the obtained values of condensed Fukui function and Voronoi deformed density derived charges, for this atom, are in line with the experimental observation. The closely related organosilicon species derived from an N-substituted diethanolamines RR'Si[(OCH$_2$CH$_2$)$_2$NR''] shows a tendency to coordinate the nitrogen atom as a consequence of stereoelectronic effects [10]. Depending on the bulkiness of R, R' and R'' substituents the interaction Si – N ranges from strong to weak and to no-interaction, according to crystallographic interatomic-distance measurements. When the R'' group on nitrogen is small (R'' = H, Me), the interaction Si – N is stronger in spite of R and R' groups bulkiness; when R'' is *tert*-butyl or phenyl, there is no interaction Si – N in spite of the presence of small R and R' groups on silicon. This suggests a more important p-character and larger basicity for the electron pair on nitrogen as the R'' group decreases in size, and the reverse is also true. In the present case it seems that there are no steric effects, as the oxygen atom has no third R group as nitrogen does.

Our DFT theoretical calculations at the BP86/TZ2P level of theory confirm that diethyleneglycol acts only as a dianionic, bidentate ligand towards silicon. This is further confirmed by the fact that harmonic analysis indicates that the tetracoordinated Si complex has only positive vibrational frequencies, i.e. it is a true energy minimum (stable molecule), while the hexacoordinated complex turns out to be a saddle point or transition state (only a single imaginary frequency is obtained). These theoretical findings are in agreement with experimental observations. This behaviour is apparently due to the fine detail in the donating-capability of the oxygen atoms and its strong dependence with the different geometries of each possible Si complex. This explains the appearance of only a spirocyclic tetracoordinated silicon complex and no evidence of formation of any hypervalent alkoxysilane. The theoretical harmonic analysis reveals that the pseudo-octahedral species is apparently a transition state, which probably connects with another tetrahedral isomer and our characterized tetracoordinated species, with a 4.39 kcal/mol activation barrier for the conversion.

We have also computed the chemical shifts (from the computed total isotropic NMR shieldings respect to the computed TMS value) over the protons and the silicon centre of the complex. In general all values are in excellent agreement with the experimental ones.

## Acknowledgements

## References

1. a) Brook, M. A. *Silicon in Organic, Organometallic and Polymer Chemistry*, 1ˢᵗ ed., Wiley, New York, **2000**; b) Wong, C. Y.; Woollins, J. D. *Coord. Chem. Rev.* **1994**, *130*, 175-1241; c) Cheng, H.; Tamaki, R.; Laine, R. M.; Babonneau, F.; Chujo, Y.; Treadwell, D. R. *J. Am. Chem. Soc.* **2000**, *122*, 10063-10072.
2. a) Davison, J. B.; Wynne, K. J. *Macromolecules* **1978**, *11*, 560-565; b) Lee, P. P. S.; Ngai, T.; Huang, J.-D.; Chi, W.; Fong, W. P.; Ng, D. K. P. *Macromolecules* **2003**, *36,* 7527-7533; c) Brus, J.; Kotlík, P. *Chem. Mater.* **1996**, *8,* 2739-2744; d) Jitianu, A.; Britchi, A.; Deleanu, C.; Badescu, V.; Zaharescu, M. *J. Non-Crystal. Sol.* **2003**, *319*, 263-279.
3. a) Tanev, P. T.; Pinnavaia, T. J. *Science* **1996**, *271*, 1267-1269; b) Ulagappan, N.; Battaram, N.; Raju, V. N.; Rao, C. N. R. *Chem. Commun.* **1996**, 2243-2244.
4. Gournis, D.; Georgakilas, V.; Karakassides, M. A.; Bakas, T.; Kordatos, K.; Prato, M.; Fanti, M.; Zerbetto, F. *J. Am. Chem. Soc.* **2004**, *126*, 8561-8568.

5. Surivet, F.; My, L. T.; Pascaultj, J.-P.; Quang, T. P. *Macromolecules* **1992**, *25*, 4309-4320.
6. a) Rosenheim, A.; Raibmans, B.; Schendel, G. *Z. Anorg. Allg. Chem.* **1931**, *196*, 160-176; b) Barnum, D. W. *Inorg. Chem.* **1972**, *11*, 1424-1429; c) Azuma, S.; Kojima, M.; Yoshikawa, Y. *Inorg. Chim. Acta* **1998**, *271*, 24-28; d) Hahn, W. *Makromol. Chem.* **1953**, *11*, 51-63; e) Müller, R.; Heinrich, L. *Chem. Ber.* **1961**, *94*, 1943-1951; f) Frye, C. L. *J. Org. Chem.* **1969**, *34*, 2496-2499; g) Frye, C. L. *J. Am. Chem. Soc.* **1970**, *92*, 1205-1210; h) Frye, C. L.; Vincent, G. A.; Finzel, W. A. *J. Am. Chem. Soc.* **1971**, *93*, 6805-6811; i) Kinrade, S. D.; Deguns, E. W.; Gilson, A. – M. E.; Knight, C. T. G. *J. Chem. Soc., Dalton Trans.* **2003**, 3713-3716.
7. a) Klüfers, P.; Benner, K.; Vogt, M. *Angew. Chem. Int. Ed.* **2003**, *42*, 1058-1062; b) Klüfers, P.; Benner, K.; Schuhmager, J. *Z. Anorg. Allg. Chem.* **1999**, *625*, 541-543; c) Lambert, J. B.; Lu, G.; Singer, S. R.; Kolb, V. M. *J. Am. Chem. Soc.* **2004**, *126*, 9611-9625.
8. a) Boudin, R.; Cerveau, G.; Chuit, C.; Corriu, R. J. P.; Reye, C. *Organometallics* **1988**, *7*, 1165-1171; b) Laine, R. M. *US Patent* 5440011
9. a) Krieble, R. H.; Burkhard, C. A. *J. Am. Chem. Soc.* **1947**, *69*, 2689-2692; b) D'yakov, V. M.; Kir'yanova, A. N.; Kireeva, L. N.; Chernyshev, A. E.; Bochkarev, V. N.; Androsenko, S. I. *Chem. Abst.* 110:23956; c) Oddon, G.; Hosseini, M. W. *Tetrahedron Lett.* **1993**, *34*, 7413-7416; d) Kupce, E.; Liepins, E.; Zicmane, I.; Lukevics, E. *Mag. Res. Chem.* **1987**, *25*, 1084-1086.
10. Kemme, A.; Bleidelis, J.; Urtane, I.; Zelchan, G.; Lukevics, E. *J. Organometal. Chem.* **1980**, *202*, 115-121.
11. Kost, D.; Kalikhman, I. *Hypervalent Silicon Compounds* in:*The Chemistry of Organic Silicon Compounds*, 1st edition, Rappoport Z. and Apeloig, Y. editors, Wiley, Chichester, **1998**, Vol. 2 part 2. Ch. 23, p. 1339.
12. Chuit, C.; Corriu, R. J. P.; Reye, C.; Young, J. C. *Chem. Rev.* **1993**, *93*, 1371-1448.
13. Kinrade, S. D.; Hamilton, R. J.; Schach, A. S.; Knight, C. T. G. *J. Chem. Soc., Dalton Trans.* **2001**, 961-963.
14. Hahn, F. E.; Keck, M.; Raymond, K.N. *Inorg. Chem.* **1995**, *34*, 1402-1407.
15. a) Parr, R. G.; Yang, W. *Density Functional Theory of Atoms and Molecules*, Breslow, R.; Goodenough, J. B.; Halpern, J.; Rowlinson J. S. eds., Oxford Univ. Press, USA, **1989**, p. 99-101; b) Dreizler, R. M.; Gross, E. K. U. *Density Functional Theory. An approach to the Quantum Many-Body Problem*, Dreizler R. M.; Gross, E. K. U. eds., Springer-Verlag, Berlin, **1990**.
16. a) Fuentealba, P.; Pérez, P.; Contreras, R. *Chem. Phys.* **2000**, *113*, 2544-2551; b) Fuentealba, P.; Contreras, R. In *Reviews of Modern Quantum Chemistry: A Celebration of the Contributions of Robert G. Parr*, K. D. Sen, ed., World Scientific, Singapore, **2002**, p. 1013 –1052

17. Baerends, E. J.; Autschbach, J. A.; Bérces, A.; Bo, C.; Boerrigter, P. M.; Cavallo, L.; Chong, D. P.; Deng, L.; Dickson, M.; Ellis, D. E.; Fan, L.; Fischer, T. H.; Fonseca Guerra, C.; van Gisbergen, S. J. A.; Groeneveld, J. A.; Gritsenko, O. V.; Grüning, M.; Harris, F. E.; van den Hoek, P.; Jacobsen, H.; van Kessel, G.; Kootstra, F.; van Lethe, E.; Osinga, V. P.; Patchkovskii, S.; Philipsen, P. H. T.; Post, D.; Pye, C. C.; Ravenek, W.; Ros, P.; Schipper, P. R. T.; Schreckenbach, G.; Snijders, J. G.; Solà, M.; Swart, M.; Swerhone, D. te Velde, G.; Vernooijs, P.; Versluis, L.; Visser, P.; van Wezenbeek, E.; Wiesenekker, G.; Wolff, S. K.; Woo, T. K.; Ziegler, T. ADF2003.01, SCM, *Theoretical Chemistry*; Vrije Universiteit: Amsterdam, **2003**.
18. Vosko, S. H.; Wilk, L.; Nusair, M. *Can. J. Phys.* **1980**, *58*, 1200-1211.
19. Becke, A. D.*Phys. Rev. A*, **1988**, *38*, 3098-3100.
20. Perdew, J. P. *Phys. Rev. B* **1986**, *33*, 8822-8824.
21. Portmann, S.; Lüthi, H. P. *Chimia* **2000**, *54*, 766 –770.
22. a) Schreckenbach, G.; Ziegler, T. *J. Phys. Chem.* **1995**, *99*, 606-611; b) Schreckenbach, G.; Ziegler, T. *Int. J. Quantum Chem.*, **1997**, *61*, 899-918; c) Wolff, S. K.; Ziegler, T. *J. Chem. Phys.* **1998**, *109*, 895-905.
23. Kemmitt, T.; Henderson, W. *Aust. J. Chem.* **1998**, *51*, 1031-1035.
24. Williams, E. A. *NMR spectroscopy of organosilicon compounds* in *The Chemistry of Organosilicon Compounds* Part 1. Edited by Patai S. and Rappoport, Z. Wiley, New York, **1989**.
25. a) Silverstein, R. M.; Bassler, G. C.; Morrill, T. C. *Spectrometric Identification of Organic Compounds*, 5th ed., John Wiley and Sons, New York, **1991**, p. 190-191. b) *ibid.* p. 15, 19.
26. Sheldrick, G. M. *SHELXS97, SHELXL97, Programs for Crystal Structure Analysis*, Institüt für Anorganische Chemie der Universität, Tammanstrasse 4, D-3400 Göttingen, Germany, 1998.
27. Farrugia, L. J. *J. Appl. Cryst.*, **1999**, *32*, 837-838.
28. Kaftori, M.; Kapon, M.; Botoshansky, M. *The Structural Chemistry of Organosilicon Compounds* in *The Chemistry of Organosilicon Compounds* Vol. 2. Edited by Z. Rappoport and Y. Apeilog. Wiley, New York, **1998** p. 181.
29. Huheey, J. E.; Keiter, E. A.; Keiter, R. L. *Inorganic Chemistry. Principles of Structure and Reactivity*, 4th ed., Harper Collins College Publishers, N ew York, **1993**, p. 292, A-30.
30. Bickelhaupt, F. M.; van Eikema Hommes, N. J. R.; Fonseca Guerra, C.; Baerends, E. J. *Organometallics* **1996**, *15*, 2923.
31. a) Parr, R. G.; Yang, W. *J. Am. Chem. Soc.* **1984**, *106*, 4049-4050; b) Geerlings, P.; De Proft, F.; Langenaeker, W. *Chem. Rev.* **2003**, *103*, 1793-1873; c) Chermette, H. *J. Comp. Chem.* **1999**, *20,* 129-154.
32. Kocher, N.; Henn, J.; Gostevskii, B.; Kost, D.; Kalikhman, I.; Engels, B.; Stalke, D. *J. Am. Chem. Soc.* **2004**, *126*, 5563-5568.